

## Improvement in Properties of Ni-B Coatings by the Addition of Mixed Oxide Nanoparticles

A. Bahgat Radwan, R. A. Shakoor\*, Anton Popelka

Center for Advanced Materials (CAM), Qatar University, 2713, Doha, Qatar

\*E-mail: [shakoor@qu.edu.qa](mailto:shakoor@qu.edu.qa)

Received: 11 June 2015 / Accepted: 8 July 2015 / Published: 28 July 2015

---

A comparison of properties of electrodeposited Ni-B and Ni-B-ZrO<sub>2</sub>-Al<sub>2</sub>O<sub>3</sub> nanocomposite coatings is presented to explain the benefits of addition of mixed nanoparticles of ZrO<sub>2</sub> and Al<sub>2</sub>O<sub>3</sub> into Ni-B matrix. A comparative study of the properties of Ni-B and Ni-B-ZrO<sub>2</sub>-Al<sub>2</sub>O<sub>3</sub> nanocomposite coatings in their as deposited condition indicates that the addition of mixed nanoparticles into Ni-B matrix has significant influence on its structural, surface, mechanical and electrochemical properties. Incorporation of mixed nanoparticles into Ni-B matrix shows significant grain refinement, substantial enhancement in mechanical properties and decent improvement in corrosion resistance. The improvement in mechanical properties can be attributed to grain refinement of Ni-B matrix and dispersion hardening effect of insoluble hard ceramic nanoparticles. Similarly, corrosion inhibition efficiency of binary Ni-B coatings is considerably improved which can be presumably regarded as the effect of formation of dense structure and decrease in active area of Ni-B matrix due to incorporation of mixed inactive nanoparticles. There is simultaneous improvement in mechanical and anti-corrosion properties of Ni-B coatings by the incorporation of mixed nanoparticles demonstrating usefulness of Ni-B-ZrO<sub>2</sub>-Al<sub>2</sub>O<sub>3</sub> nanocomposite coatings for many applications.

---

**Keywords:** coatings, electrodeposition, grain refinement, roughness, hardness, corrosion

### 1. INTRODUCTION

A large number of industries are suffering from severe corrosion problems. The corrosion of components in service not only raise the maintenance cost and lessen the plant efficiency but also result in serious safety issues. The combined effect of these two harmful processes may also lead to rapid degradation of materials making the situation even more adverse. Since, in many applications only the surface of the components undergoes chemical attack or mechanical action; therefore,

modifying surface properties in such conditions, applying different kinds of coatings is quite economical and feasible choice rather than improving the properties in the bulk material[1].

Ni-B coatings are now receiving substantial attention due to their promising characteristics like high hardness and good wear properties. Additionally, Ni-B coatings also possess uniform thickness, less porosity, decent ductility, good electrical and magnetic properties. These appealing properties of Ni-B coatings make them suitable to petrochemical, automotive, aerospace and many other industries [2-6]. Although, Ni-B coatings have some promising properties such as high hardness and wear. However, improvement in their properties is vital to expand their utility to more challenging requirements [7].

The properties of binary Ni-B coatings have been improved by the addition of alloying elements such as cobalt[8-10] and Zinc [7]. At the same time addition of insoluble hard second phase particles has also resulted in improvement in properties of Ni-B coatings. These second phase particles are  $\text{TiO}_2$ [8],  $\text{Si}_3\text{N}_4$ [9, 10],  $\text{Al}_2\text{O}_3$ [11],  $\text{CeO}_2$ [1], diamond (C) [12], and  $\text{ZrO}_2$ [13]. It is pertinent to mention here that each alloying element and a second phase particle addition have a specific role in improving the properties of binary Ni-B coatings. For instance, the addition of cobalt has resulted in improvement in the magnetic properties [14] whereas addition of zinc into Ni-B improves hardness and corrosion resistance. Similarly, incorporation of  $\text{Al}_2\text{O}_3$  [11] improves mechanical properties and the corrosion resistance of binary Ni-B coatings. Many types of substrates including mild steel, Mg-alloy, Al-alloys, stainless steels and copper have been coated using either nickel electroless or nickel electrodeposition coating process. As a comparison, electroless coating process has been mostly used in the previous studies for the development of Ni-B coatings [1, 5, 7, 11]. However, electrodeposition process is also becoming popular to synthesize Ni-B coatings due to its salient advantages such as low cost, high purity of the deposit formed, large production rate, no shape limitations, capable of processing a range of substrates (metals, ceramics and polymers), controlled composition and its ability to synthesize coatings on nanometric scale [15-17]. Electrodeposition coating bath solution usually comprised of source of nickel ( $\text{NiSO}_4$  and  $\text{NiCl}_2$ ), a complexing agent ( $\text{H}_3\text{BO}_3$ ) and a reducing agent. Different types of reducing agents have been employed for electrodeposition of binary Ni-B coatings which mainly comprises of potassium borohydride [18], dimethylamine borane[9, 10, 13], trimethylamine borane [19], carborane ion[15] and sodium decahydrodecaborate [15, 20]. However, developing Ni-B coatings using dimethyl amine borane is more popular.

It is useful to achieve the most desired properties by incorporating two or more different kinds of ceramic particles into the soft matrix. Some reports addressing the effect of mixed second phase particles on the properties of Ni-P coatings have been published earlier which include Ni-P- $\text{Fe}_2\text{O}_3$ - $\text{TiO}_2$ [21], Ni-P- $\text{TiO}_2$ - $\text{RuO}_2$ [22], Ni- $\text{Al}_2\text{O}_3$ -SiC [23] etc. To the best of our knowledge, effect of addition of mixed  $\text{ZrO}_2$  and  $\text{Al}_2\text{O}_3$  nanoparticles on the properties of Ni-B binary coatings is not reported so far. This will be the first report addressing the effect of incorporation of mixed oxides nanoparticles on the properties of binary Ni-B coatings.

The present research work emphasizes on novel Ni-B- $\text{ZrO}_2$ - $\text{Al}_2\text{O}_3$  nanocomposite coatings which have been deposited on mild steel substrates through conventional electrodeposition process by adding nano sized  $\text{ZrO}_2$  and  $\text{Al}_2\text{O}_3$  into Ni-B matrix to gain the combined benefits of  $\text{ZrO}_2$  and  $\text{Al}_2\text{O}_3$ . A comparative study of binary Ni-B and Ni-B- $\text{ZrO}_2$ - $\text{Al}_2\text{O}_3$  nanocomposite coatings indicates that the

incorporation of mixed nanoparticles of  $ZrO_2$  and  $Al_2O_3$  into Ni-B matrix has a significant influence on its structural, surface, mechanical and corrosion properties. It is noticed that co-deposition of  $ZrO_2$  and  $Al_2O_3$  into Ni-B matrix results in significant grain refinement and simultaneous improvement in hardness and corrosion behavior. Explanations for the improvement in the properties of binary Ni-B matrix by the addition of mixed nanoparticles have been provided. Owing to their superior properties, we feel that Ni-B- $ZrO_2$ - $Al_2O_3$  nanocomposite coatings can be well suited to meet the challenging requirements of oil, gas, sea water desalination, automobile and many other related industries.

## 2. EXPERIMENTAL

Ni-B and Ni-B- $ZrO_2$ - $Al_2O_3$  nanocomposite coatings were deposited on mild steel substrates having a size of 30 X 30 X1.5 mm. All substrates were mechanically ground using different SiC papers (220, 320, 500, 800, 1000, 1200) to remove any contamination present and to achieve a flat mirror like surface. After mechanical cleaning all substrates were further cleaned with alkaline solution and acetone. The substrates were then thoroughly washed with distilled water and their surfaces were activated with 20 % solution of HCl for about one minute. After activating the prepared surface, the substrates were thoroughly rinsed and were coated through electrodeposition process. The coating solution and experimental details for the synthesis of Ni-B and Ni-B- $ZrO_2$ - $Al_2O_3$  nanocomposite coatings are presented in Table 1. A pure nickel sheet and mild steel sheet (substrate) were used as anode and cathode respectively. The coatings were synthesized at  $53 \pm 1^\circ C$  for a fixed deposition time of 30 minutes. The solution was constantly rotated with a magnetic stirrer at 500 rpm to have uniform coating. The Ni-B- $ZrO_2$ - $Al_2O_3$  nanocomposite coatings were synthesized by adding nanoparticles of  $ZrO_2$  and  $Al_2O_3$  into the coating bath. The compositional analysis was carried out through Inductively Coupled Plasma-Mass Spectroscopy (ICP-MS-NexIon-300D, PerkinElmer, USA) and Energy Dispersive X-Ray Spectroscopy (EDX). The composition of nickel and boron was obtained with ICP whereas the amount of second phase nanoparticles ( $ZrO_2$  and  $Al_2O_3$ ) was analyzed with EDX. The structure of the coatings was studied with X-Ray diffractometer (XRD, Rigaku, Miniflex2 Desktop, Tokyo, Japan) using Cu  $K\alpha$  radiations. The coating morphology and its surface analysis were carried out through field emission scanning electron microscope (FE-SEM, Nova Nano-450, Netherland) and atomic force microscopy (AFM, USA). The detailed procedure can be found in our previous report [1]. The mechanical properties of the developed coatings were measured with Vickers Micro Hardness Tester (FM-ARS9000, USA) and MFP-3D NanoIndenter (head connected to AFM equipment) with Standard tip indenter having spring constant of 4000 N/m. The indentation was performed with Berkovich diamond indenter tip using maximum 1mN indentation force (loading and unloading rate: 200  $\mu N/s$  and dwell time at maximum load: 5s). The Oliver and Pharr method was used to determine the contact penetration from the unloading curve.

The corrosion resistance of synthesized coatings in their as electrodeposited state was investigated by Potentiodynamic linear polarization technique employing Gamary 3000 (30K BOOSTER potentiostat/Galvanstate/ZRA, USA). All tests were performed at room temperature ( $25^\circ C$ ), in 3.5 wt.% NaCl aqueous solution, using conventional triple electrode cell comprising of a

working electrode (substrate-mild steel sheet), saturated calomel reference electrode and a graphite counter electrodes. In all measurements the exposed area of the test sample was kept fixed to 0.785 cm<sup>2</sup>. All tests samples were scanned at of 0.167 mV sec<sup>-1</sup>.

**Table 1.** Composition and operating conditions for electrodeposition of coatings.

No	Nomenclature	Composition
1	Nickel sulphate hexa hydrate	240g/l
2	Nickel chloride hexa hydrate	45g/l
3	Boric acid	30g/l
4	Dimethylamine borane complex (DMAB)	3g/l
5	ZrO <sub>2</sub> +Al <sub>2</sub> O <sub>3</sub> nano powder	(4.5+4.5) g/l
1	pH	4 ± 0.1
2	Temperature	53±1 °C
3	Coating time	30 minutes
4	Current	50 mA/cm <sup>2</sup>
5	Coating solution stirring	500 rpm

### 3. RESULTS AND DISCUSSION

#### 3.1. Incorporation of boron and oxide nanoparticles

The incorporation of boron (B) and nanoparticles of ZrO<sub>2</sub> and Al<sub>2</sub>O<sub>3</sub> was confirmed by ICP and EDX analysis respectively. The contents of boron in binary Ni-B and Ni-B-ZrO<sub>2</sub>-Al<sub>2</sub>O<sub>3</sub> nanocomposite coatings were determined with ICP analysis as EDX analysis does not give accurate value of boron. The ICP compositional analysis of binary Ni-B coatings indicates that the addition of DMAB into nickel plating solution (Watts solution bath) has resulted in successful co-deposition of boron (7.7 at. %) with nickel (Ni) forming Ni-B coatings. The incorporation of boron into nickel matrix takes place through adsorption and decomposition processes. During the adsorption process, DMAB was first adsorbed on the surface of freshly deposited nickel and is then converted into pure boron through decomposition process [3].

The EDX results of Ni-B and Ni-B-ZrO<sub>2</sub>-Al<sub>2</sub>O<sub>3</sub> nanocomposite coatings in as deposited state are presented in Figure 1 (a, b). The presence of peaks of zirconium (Zr) and aluminum (Al) in the EDX analysis of Ni-B-ZrO<sub>2</sub>-Al<sub>2</sub>O<sub>3</sub> nanocomposite (Figure 1 (b)) confirms the successful co-deposition of ZrO<sub>2</sub> and Al<sub>2</sub>O<sub>3</sub> nanoparticles in the Ni matrix along with boron (B). Our EDX analysis indicates that mixed nanoparticles like ZrO<sub>2</sub> and Al<sub>2</sub>O<sub>3</sub> can be incorporated into Ni-B matrix using acidic coating conditions. The co-deposition of nanoparticles of ZrO<sub>2</sub> (1.2 at.%) and Al<sub>2</sub>O<sub>3</sub> (2.7 at.%) into nickel layer can take place possibly through three mechanisms namely (i) mechanical interlocking (ii) electrophoresis and (iii) adsorption of nanoparticles onto the surface of cathode by Vander Waals attractive forces. During the first step, nanoparticles are attached to nickel ions due to mechanical interlocking. In the second step, nanoparticles attached to nickel ions move towards the cathode

surface because of electrophoresis. In the third step nano particles adsorb onto the cathode surface due to adsorption and subsequent reduction of nickel ions at the cathode surface resulted in encapsulation and incorporation of nanoparticles into Ni-B matrix. This mode of addition of insoluble hard ceramics has also been reported in some previous studies [1, 9, 11]. The incorporation of insoluble hard ceramic particles such as  $\text{Si}_3\text{N}_4$ [9],  $\text{CeO}_2$ [1],  $\text{Al}_2\text{O}_3$ [11],  $\text{TiO}_2$ [8] and  $\text{ZrO}_2$ [13] into Ni-B matrix using acidic solution bath conditions has also been reported in earlier reports.

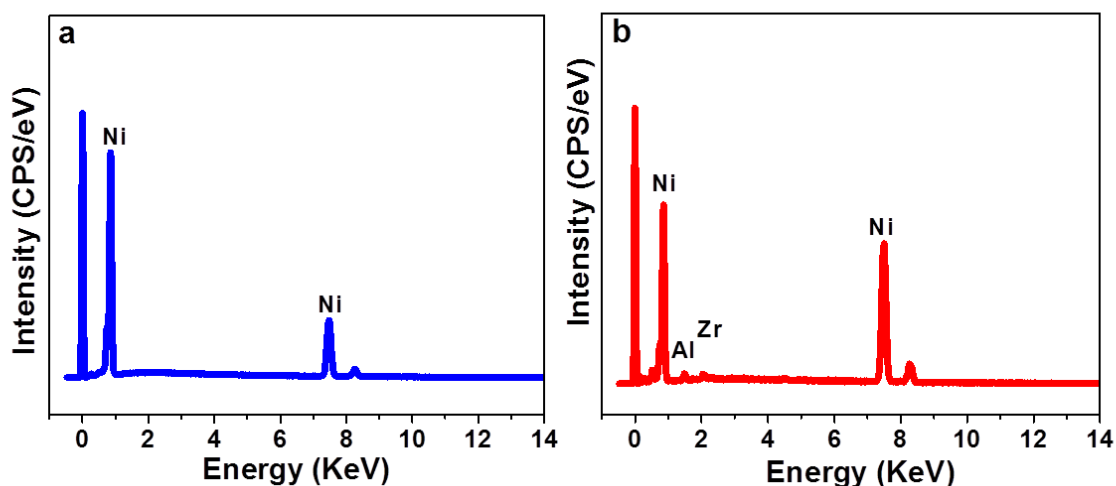


**Figure 1.** EDX results of coatings in their as deposited state (a) Ni-B (b) Ni-B-ZrO<sub>2</sub>-Al<sub>2</sub>O<sub>3</sub> nanocomposite coatings.

### 3.2. Structural analysis

The crystal structure and purity of the phases formed in the synthesized coatings in their as deposited state was conducted with XRD. A comparative analysis of XRD spectra of substrate, Ni-B and Ni-B-ZrO<sub>2</sub>-Al<sub>2</sub>O<sub>3</sub> nanocomposite coatings presented in Figure 2 reveals that Ni-B coating exhibits a broad peak representative of Ni (111) reflections. The existence of only one broad peak of Ni (111) shows that Ni-B coatings in their as deposited state are amorphous. In fact, the crystal structure of Ni-B coatings is susceptible to the coating composition, grain size and heat treatment process. Ni-B coating can be crystalline or amorphous based upon the amount of boron present. At the same time the reduction in grain size also leads to amorphous character of the coatings.

It is pertinent to mention here that Ni-B coatings having about 8 at. % boron show significant broadening of Ni (111) peak at the expense of other peaks and thus demonstrate a complete amorphous nature of the coating structure. The existence of only one broad Ni (111) peak in XRD pattern confirms the amorphous nature of the Ni-B coatings in their as electrodeposited state which satisfies the ICP results and the earlier works [24-27]. Similarly, the XRD spectrum of Ni-B-ZrO<sub>2</sub>-Al<sub>2</sub>O<sub>3</sub> nanocomposite coating also shows one main Ni (111) peak similar to binary Ni-B coatings depicting amorphous nature of the coatings.

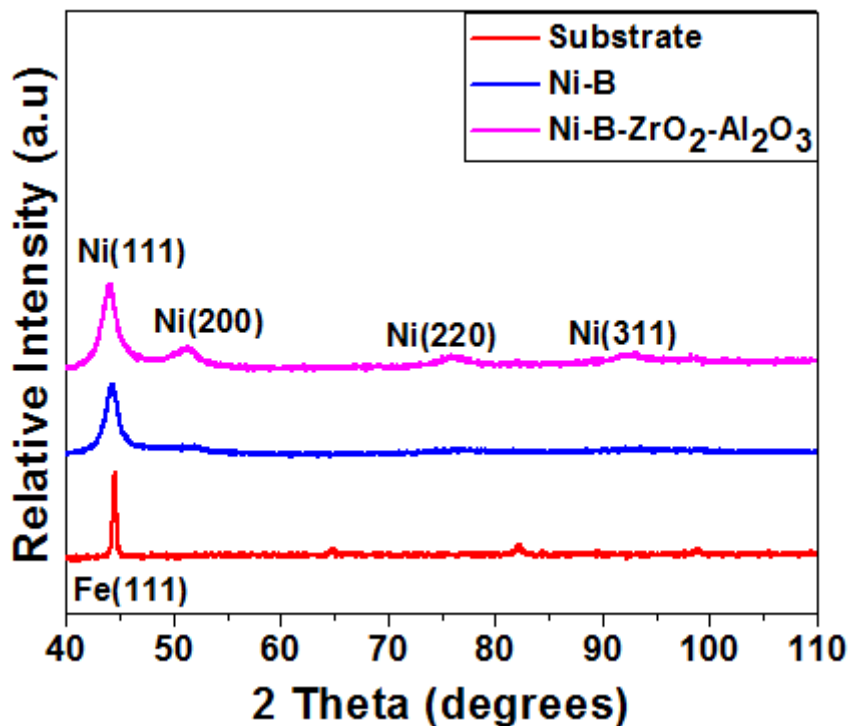


**Figure 2.** XRD analysis of substrate, Ni-B and Ni-B-ZrO<sub>2</sub>-Al<sub>2</sub>O<sub>3</sub> nanocomposite coatings in their as deposited state.

However, the presence of additional peaks of Ni (200), Ni (220) and Ni (311) in the XRD spectrum suggests that the incorporation of nanoparticles of ZrO<sub>2</sub> and Al<sub>2</sub>O<sub>3</sub> has resulted in improvement in crystallinity of the binary Ni-B coatings. It is well reported that addition of insoluble hard ceramic particles into Ni-B matrix has significant influence on its chemical composition, crystal structure, surface roughness, mechanical and corrosion behavior [10]. As a comparison the effect of addition of nanoparticles of ZrO<sub>2</sub> and Al<sub>2</sub>O<sub>3</sub> in improving crystallinity of Ni-B coatings is less pronounced when compared to the same oxide particles incorporated into Ni-B matrix in micron size to form composite coatings of Ni-B-Al<sub>2</sub>O<sub>3</sub> [11] and Ni-B-ZrO<sub>2</sub> [13] due to inherent amorphous nature of nanoparticles.

### 3.3. Surface analysis

Figure 3 (a, b) shows the surface morphology of Ni-B and Ni-B-ZrO<sub>2</sub>-Al<sub>2</sub>O<sub>3</sub> nanocomposite coatings in as synthesized state. A comparative study of SEM images reveals that both coatings are made up of homogenous, uniform and fine grained structures. The presence of nanoparticles of ZrO<sub>2</sub> and Al<sub>2</sub>O<sub>3</sub> into the structure is too visible (Fig. 3 (c)). A typical cauliflower structure is obtained which is considered useful for tribological applications as it can retain lubricants in the pockets and thus reduces the wear. In addition, the formation of dense and pore free coatings retards the corrosion phenomenon by preventing the penetration of the solvent to attack the substrate.

A comparison of SEM images presented in Figure 3 (a, b) also clearly reveals that incorporation of nanoparticles of  $ZrO_2$  and  $Al_2O_3$ , has resulted in significant grain refinement of the Ni-B matrix. This refinement in grain size is quite desired as the fine grained structure of coatings leads to enhance the mechanical properties.

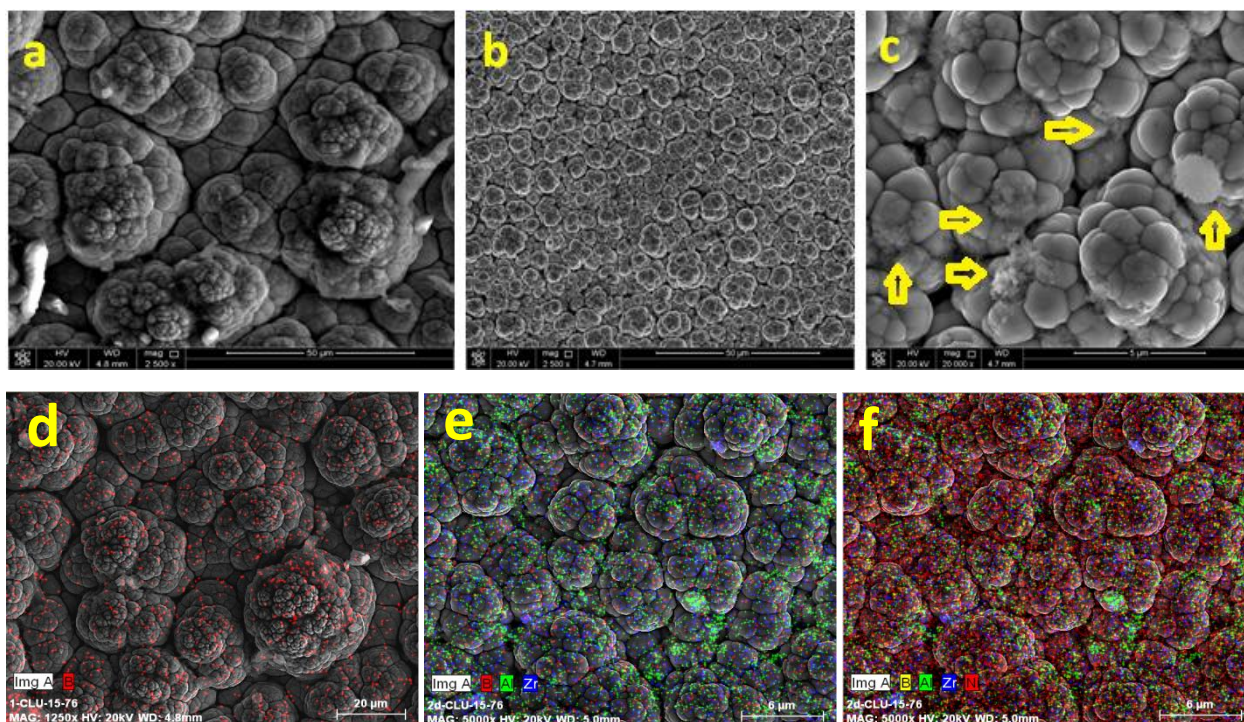


**Figure 3.** (a) SEM analysis of coatings in their as deposited state (a) Ni-B coatings (b) Ni-B- $ZrO_2$ - $Al_2O_3$  nanocomposite coatings (c) Ni-B- $ZrO_2$ - $Al_2O_3$  nanocomposite coatings showing presence of nanoparticles (d) boron distribution in Ni-B coatings (e) distribution of boron, zirconia and alumina in Ni-B- $ZrO_2$ - $Al_2O_3$  nanocomposite coatings (f) distribution of nickel, boron, zirconia and alumina in Ni-B- $ZrO_2$ - $Al_2O_3$  nanocomposite coatings.

The formation of fine grain structure in Ni-B- $ZrO_2$ - $Al_2O_3$  nanocomposite coatings as compared to binary Ni-B coatings can be attributed two factors; (1) increase of electro crystalline potential due to the reduction in surface area of cathode and (2) prevention of grain growth due to the presence of nanoparticles at the cathode surface [1, 11, 13, 28]. The SEM elemental mapping images of Ni-B and Ni-B- $ZrO_2$ - $Al_2O_3$  nanocomposite coatings are also shown in Figure 3 (d, e, f), to demonstrate the presence and distribution of different constituents of coatings comprising of nickel (Ni), boron (B), zirconium dioxide ( $ZrO_2$ ) and alumina ( $Al_2O_3$ ) particles. In order to examine the coating thickness a cross-section of the synthesized Ni-B and Ni-B- $ZrO_2$ - $Al_2O_3$  nanocomposite coatings were studied by SEM. Figure 4 shows SEM image of Ni-B- $ZrO_2$ - $Al_2O_3$  nanocomposite coatings. It can be noticed that Ni-B- $ZrO_2$ - $Al_2O_3$  nanocomposite coatings show a compact structure having no defects at the substrate/coating interface indicating good bonding between the coating and the substrate. The average coating thickness was about  $34 \pm 2$  and  $32 \pm 1$   $\mu m$  for Ni-B and Ni-B- $ZrO_2$ - $Al_2O_3$  coatings, respectively.

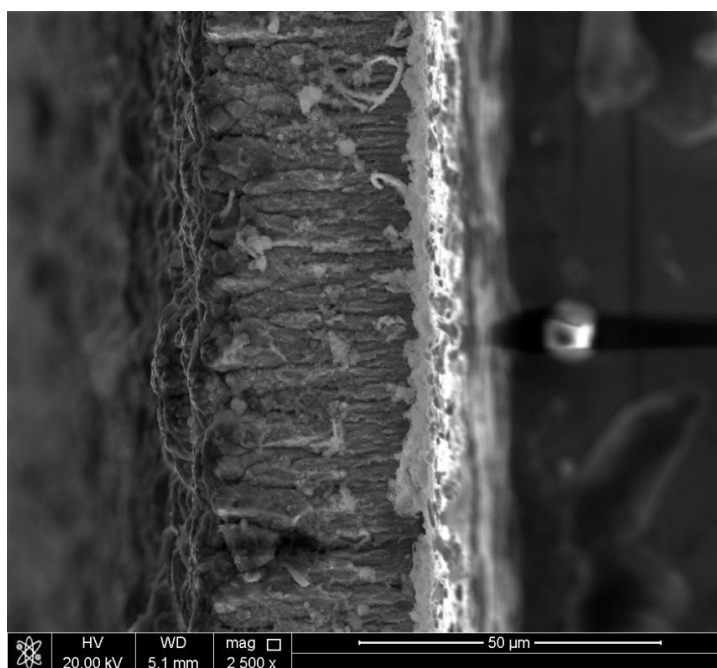


**Figure 4.** SEM image of cross-section of Ni-B-ZrO<sub>2</sub>-Al<sub>2</sub>O<sub>3</sub> nanocomposite coating.

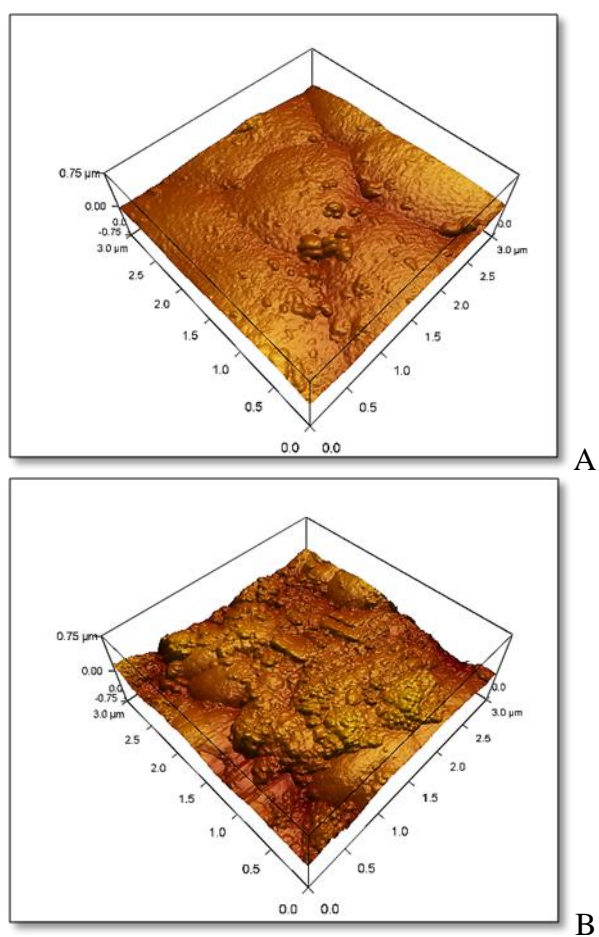


**Figure 5.** 3D AFM images of coatings in their as deposited condition (a) Ni-B and (b) Ni-B-ZrO<sub>2</sub>-Al<sub>2</sub>O<sub>3</sub> nanocomposite coatings.

A more detailed surface examination of synthesized coatings in their as deposited condition was carried out using AFM. A comparison of 3D images of coatings shown in Figure 5 (a, b) indicates that the surface of Ni-B-ZrO<sub>2</sub>-Al<sub>2</sub>O<sub>3</sub> nanocomposite coatings (Figure 5 (b) is more rough as compared to Ni-B coatings Figure 5 (a). The presence of nanoparticles of ZrO<sub>2</sub> and Al<sub>2</sub>O<sub>3</sub> in the Ni-B matrix can also be clearly seen in Ni-B-ZrO<sub>2</sub>-Al<sub>2</sub>O<sub>3</sub> nanocomposite coatings (Figure 5 (b)). The increase in surface roughness of Ni-B binary coatings may presumably regarded as the effect of presence of nanoparticles of ZrO<sub>2</sub> and Al<sub>2</sub>O<sub>3</sub> in the Ni-B matrix.

A quantitative analysis of surface roughness of coatings in their as synthesized condition was also conducted. The AFM images of Ni-B and Ni-B-ZrO<sub>2</sub>-Al<sub>2</sub>O<sub>3</sub> nanocomposite coatings with their surface line profiles are illustrated in Figure 6 (a, b). The surface roughness of coatings (R<sub>a</sub>) was measured from surface line profiles. A comparison of surface line profiles of both the coatings indicates that Ni-B coatings have smooth and uniform surface as compared to Ni-B-ZrO<sub>2</sub>-Al<sub>2</sub>O<sub>3</sub> nanocomposite coatings. The R<sub>a</sub> of Ni-B is found to be 45.0 nm whereas the R<sub>a</sub> value for Ni-B-ZrO<sub>2</sub>-Al<sub>2</sub>O<sub>3</sub> nanocomposite coatings is 110.0 nm which is significantly higher than Ni-B coatings. The AFM surface analysis of both coatings reveals that the addition of nanoparticles of ZrO<sub>2</sub> and Al<sub>2</sub>O<sub>3</sub> into Ni-B matrix leads to increase in surface roughness. This is understood as the existence of nanoparticles of ZrO<sub>2</sub> and Al<sub>2</sub>O<sub>3</sub> into the Ni-B matrix hinders the free movement of the AFM tip. These results are also in agreement with earlier works [1, 11, 13].

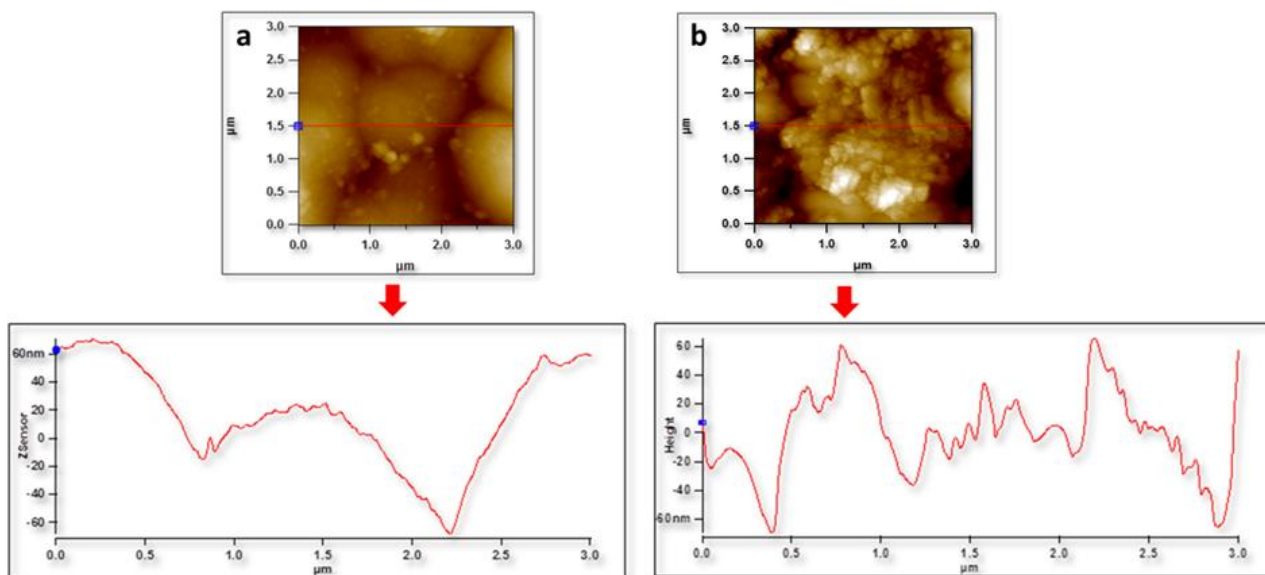


**Figure 6.** AFM images and surface line profiles of coatings in their as deposited state (a) Ni-B coatings (b) Ni-B-ZrO<sub>2</sub>-Al<sub>2</sub>O<sub>3</sub> nanocomposite coatings.

### 3.4 Mechanical properties

The hardness of Ni-B and Ni-B-ZrO<sub>2</sub>-Al<sub>2</sub>O<sub>3</sub> nanocomposite coatings was determined in their as deposited state to study the effect of incorporation of nanoparticles of ZrO<sub>2</sub> and Al<sub>2</sub>O<sub>3</sub> on the mechanical properties of binary Ni-B coatings. The microhardness of coatings was determined with

Vickers micro hardness tester and the results are presented in Figure 7. The hardness of substrate is also presented for a clear comparison purpose. The hardness results are based on the average of five readings.

It can be noticed that the hardness of substrate is ~HV 100. The hardness of binary Ni-B coating is ~HV 800.0. The hardness of Ni-B-ZrO<sub>2</sub>-Al<sub>2</sub>O<sub>3</sub> nanocomposite coating is ~HV 1300. There is an improvement of ~63% in the hardness of Ni-B coatings when nanoparticles of ZrO<sub>2</sub> and Al<sub>2</sub>O<sub>3</sub> are incorporated into binary Ni-B matrix. This indicates that the hardness of binary Ni-B coatings is remarkably increased by reinforcing Ni-B matrix with second phase nanoparticles like ZrO<sub>2</sub> and Al<sub>2</sub>O<sub>3</sub>.

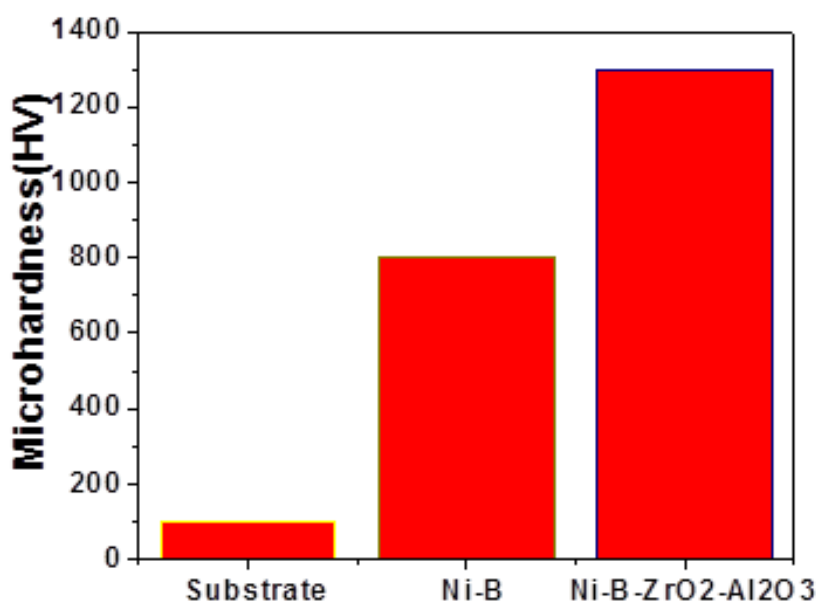


**Figure 7.** Hardness comparison of substrate, Ni-B and Ni-B-ZrO<sub>2</sub>-Al<sub>2</sub>O<sub>3</sub> nanocomposite coatings in their as synthesized condition.

In order to have more insight of the effect of addition of mixed nanoparticles on mechanical properties of Ni-B coatings, nanoindentation experiments were conducted on Ni-B and Ni-B-ZrO<sub>2</sub>-Al<sub>2</sub>O<sub>3</sub> nanocomposite coatings. Figure 8 represents the nanoindentation results of Ni-B and Ni-B-ZrO<sub>2</sub>-Al<sub>2</sub>O<sub>3</sub> nanocomposite coatings in their as synthesized condition. A comparative study of loading and unloading profiles indicates that the indentation depth of Ni-B-ZrO<sub>2</sub>-Al<sub>2</sub>O<sub>3</sub> nanocomposite coatings is small as compared to Ni-B coatings. This result shows that Ni-B-ZrO<sub>2</sub>-Al<sub>2</sub>O<sub>3</sub> nanocomposite coatings have high hardness which is consistent with our microhardness results. For more clarity a quantitative analysis of nanoindentation results (Force versus indentation depth) was conducted and mechanical properties of coatings were calculated from their corresponding loading-unloading profiles (Table 2).

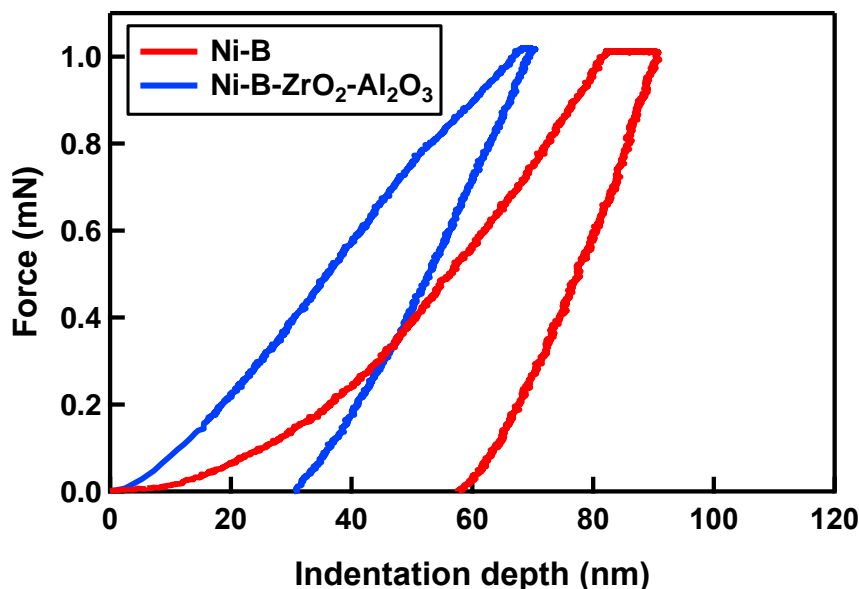


**Figure 8.** Nanoindentation results of Ni-B and Ni-B-ZrO<sub>2</sub>-Al<sub>2</sub>O<sub>3</sub> nanocomposite coatings in as deposited condition.

**Table 2.** Nanomechanical properties of coatings in their as deposited condition.

Coating	Hardness (GPa)	Modulus of elasticity (GPa)	Stiffness (KN/ m)	Plasticity
Ni-B	8.80	98.09	38.90	0.91
Ni-B-ZrO <sub>2</sub> -Al <sub>2</sub> O <sub>3</sub>	15.05	115.69	34.72	0.05

The hardness of coatings (H) was determined with the Oliver Pharr method which is given as;  $H = F_{max} / A$ , where (A) is the area =  $24.5 * H_c^2$  and  $F_{max}$  is maximum load applied (1.0 mN). Similarly, the elastic modulus (E) of the coatings was determined from  $1/E_r = (1-\nu^2)/E + (1-\nu_i^2)/E_i$  in which “E<sub>r</sub>” is reduced modulus, “ν” Poisson’s ratio of specimen (0.31), “E” Young’s modulus of coating, “ν<sub>i</sub>” Poisson’s ratio of indenter (0.2) and “E<sub>i</sub>” Young’s modulus of indenter.

The comparison of nanoindentation results presented in Table 2 indicates that the hardness of Ni-B coatings is considerably enhanced by the addition of nanoparticles of ZrO<sub>2</sub> and Al<sub>2</sub>O<sub>3</sub> which validates our microhardness results presented in Figure 7. However, our nanoindentation hardness values show a slight higher trend. Similarly, there is also increase in modulus of elasticity of Ni-B coatings by the addition of nanoparticles of ZrO<sub>2</sub> and Al<sub>2</sub>O<sub>3</sub> due to decrease in indentation depth. However, stiffness and plasticity of Ni-B-ZrO<sub>2</sub>-Al<sub>2</sub>O<sub>3</sub> nanocomposite coatings are decreased as compared to Ni-B coatings. The improvement in hardness and modulus of elasticity by the incorporation of second phase is also in agreement with earlier studies [1, 8-11, 13].

The improvement in mechanical properties of Ni-B matrix notably the hardness by the addition of nanoparticles of ZrO<sub>2</sub> and Al<sub>2</sub>O<sub>3</sub> can be attributed to grain refinement of Ni-B matrix and dispersion hardening effect of added mixed nanoparticles. The presence of insoluble, hard nanoparticles of ZrO<sub>2</sub> and Al<sub>2</sub>O<sub>3</sub> obstructs the movement of the dislocations. The pinning of dislocations at the hard

nanoparticles results in improvement in hardness. That is why, usually the addition of second particles results in blocking of dislocation movement and thus significant improvement in hardness. This improvement in hardness by the incorporation of second phase hard particles is also consistent with the previous studies [1, 9, 11, 29].

### 3.5 Potentiodynamic polarization study

The corrosion behavior of synthesized coatings was studied in 3.5 % NaCl aqueous solution and the results are illustrated in Figure 9. The values of  $E_{corr}$  and  $i_{corr}$  determined from Figure 9 are also shown in Table 3 for more clarity. The linear segments of the anodic and cathodic curves were extrapolated to corrosion potential to calculate the corrosion current densities. The slopes of these linear segments were used to calculate Tafel slopes, see Table 3. The corrosion current densities ( $i_{corr}$ ) for substrate, Ni-B and Ni-B-ZrO<sub>2</sub>-Al<sub>2</sub>O<sub>3</sub> nanocomposite coatings are 31.0  $\mu\text{A}\cdot\text{cm}^{-2}$ , 24.0  $\mu\text{A}\cdot\text{cm}^{-2}$  and 9.7  $\mu\text{A}\cdot\text{cm}^{-2}$  respectively. It is observed that incorporation of ZrO<sub>2</sub> and Al<sub>2</sub>O<sub>3</sub> results in improvement in corrosion resistance of Ni-B coatings as the value  $i_{corr}$  is lower for Ni-B-ZrO<sub>2</sub>-Al<sub>2</sub>O<sub>3</sub> nanocomposite coatings when compared to Ni-B and substrate.

The corrosion protection ( $\eta$ ) of the synthesized coatings was calculated by applying the following relationship [32].

$$\eta = 1 - \frac{i_2}{i_1} \times 100\%$$

Where  $i_1$  and  $i_2$  correspond to the corrosion current densities of the substrate and the coated samples correspondingly. The corrosion protection of Ni-B-ZrO<sub>2</sub>-Al<sub>2</sub>O<sub>3</sub> nanocomposite coatings is about 60% higher than Ni-B coatings which confirms that the addition of nanoparticles of ZrO<sub>2</sub> and Al<sub>2</sub>O<sub>3</sub> improves the corrosion resistant of the Ni-B matrix.

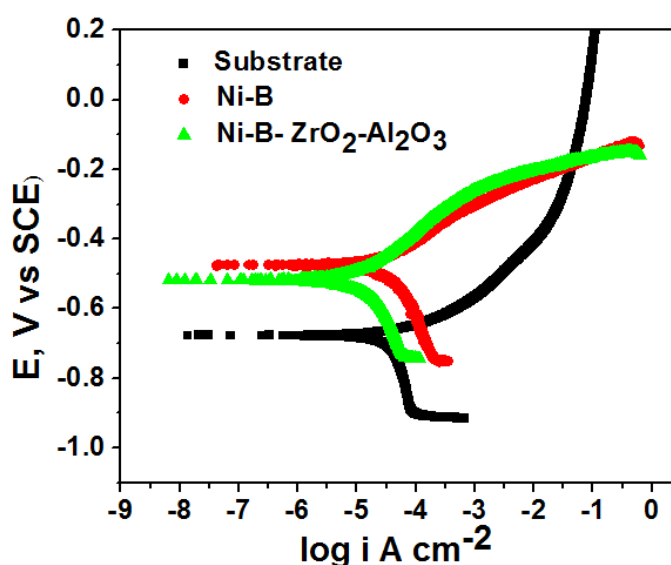


**Figure 9.** Potentiodynamic curves of Ni-B and Ni-B-ZrO<sub>2</sub>-Al<sub>2</sub>O<sub>3</sub> nanocomposite coatings in their as deposited condition in 3.5 % NaCl aqueous solution.

The enhancement in anti-corrosion properties of Ni-B ZrO<sub>2</sub>-Al<sub>2</sub>O<sub>3</sub> coatings can be attributed to the decrease in active area of Ni-B matrix due to the existence of inert of ZrO<sub>2</sub> and Al<sub>2</sub>O<sub>3</sub> nanoparticles acting as dielectric phase in the Ni-B matrix which reduce the adsorption of Cl<sup>-</sup> ions onto the exposed area. On the other hand, binary Ni-B displays less corrosion resistance due to the presence of pores which act as active sites for initiation of pitting corrosion. These results also match well with earlier reports[14, 16].

**Table 3.** Calculated corrosion results of substrate, Ni-B and Ni-B-ZrO<sub>2</sub>-Al<sub>2</sub>O<sub>3</sub> nanocomposite coatings in their as deposited state.

Nomenclature	$E_{\text{corr}}$ (mV)	$I_{\text{corr}}$ ( $\mu\text{A}$ )	$\beta_a$ mVdec <sup>-1</sup>	$\beta_c$ mVdec <sup>-1</sup>	Protection% ( $\eta$ )
Substrate	-0.670	31	57	551	-
Ni-B	-0.478	24	60	80	22
Ni-B-ZrO <sub>2</sub> -Al <sub>2</sub> O <sub>3</sub>	-0.518	9.7	124	192	86

To summarize our results and discussion, it can be stated that addition of mixed nanoparticles into Ni-B matrix has significant influence on its structure, morphology, surface, mechanical and anticorrosion properties. can say that there is significant improvement in mechanical properties Interestingly Ni-B-ZrO<sub>2</sub>-Al<sub>2</sub>O<sub>3</sub> nanocomposite coatings demonstrate simultaneous improvement in two antagonist properties of hardness and corrosion which make them attractive for many challenging applications. Owing to superior mechanical and anticorrosion characteristics of novel Ni-B-ZrO<sub>2</sub>-Al<sub>2</sub>O<sub>3</sub> nanocomposite coatings, it is anticipated that these can be well suited to oil, gas, seawater desalination, automobile and many other industries.

#### 4. CONCLUSIONS

It is concluded that mixed nanoparticles (ZrO<sub>2</sub> and Al<sub>2</sub>O<sub>3</sub>) can be co-deposited into Ni-B matrix using acidic solution bath formulation. The addition of mixed nanoparticles into Ni-B matrix results in significant grainrefinement, improvement in hardness and anti corrosion properties. The improvement in hardness can be attributed to garinrefinement of Ni-B matrix and dispersion hardening effect of the added nanoparticles. The improvement in anticorrosion properties can be regarded as the effect formation of dense structure and reduction in active area of Ni-B matrix by the presence of inactive oxide nanoparticles. There is simultanelously improvement in mechanical and anticorrosion properties of Ni-B coatings by the addition of mixed nanoparticles. The novel Ni-B-ZrO<sub>2</sub>-Al<sub>2</sub>O<sub>3</sub> nanocomposite coatings demonstrate superior mechanical and anticorrosion properties and thus can be attarctive for oil, gas, sea water desalination, automobile and many other industries.

## ACKNOWLEDGEMENTS

All authors greatly acknowledge the Center for Advanced Materials (CAM), Qatar University, 2713 Doha, Qatar for providing financial support to conduct this research work.

## References

1. R.A. Shakoor, R. Kahraman, U. S. Waware, Y. Wang, W. Gao, *Mater. Des.*, **59** (2014) 421-429.
2. I. Baskaran, R. Sakthi Kumar, T.S.N. Sankara Narayanan, A. Stephen, *Surf. Coat. Technol.*, **200** (2006) 6888-6894.
3. K. Krishnaveni, T.S.N. Sankara Narayanan and S.K. Seshadri, *Mater. Chem and Phys.*, **99** (2006) 300-308.
4. F. Delaunois, J.P. Petitjean, P. Lienard, M. Jacob-Duliere, *Surf. Coat Technol.*, **124** (2000) 201-209.
5. F. Delaunois and P. Lienard, *Surf. Coat. Technol.*, **160** (2002) 239-248.
6. A. Contreras, C. León, O. Jimenez, E. Sosa, R. Pérez, *Appl. Surf. Sci.*, **253** (2006) 592-599.
7. R. A. Shakoor, R.K. Umesh, S. Waware, Yuxin Wang and Wei Gao, *Int. J. Electrochem. Sci.*, **9** (2014) 5520-5536.
8. T.S.N. Sankara Narayanan, A. Stephan and S. Guruskanthan, *Surf. Coat. Technol.*, **179** (2004) 56-62.
9. S.A. Gamboa, J.G. Gonzalez-Rodriguez, E. Valenzuela, B. Campillo, P.J. Sebastian, *Electrochim. Acta.*, **51** (2006) 4045-4051.
10. S. Wang, *Thin Solid Films.*, **515** (2007) 8419-8423.
11. Y. Wang, S.J. Wang, X. Shu, W. Gao, W. Lu, B. Yan, *J. Alloys Compd.*, **617** (2014) 472-478.
12. K. Krishnaveni, T.S.N. Sankara Narayanan and S.K. Seshadri, *J. Alloys Compd.*, **466** (2008) 412-420.
13. K. Krishnaveni, T.S.N.S. Narayanan and S.K. Seshadri, *J. Alloys Compd.*, **480** (2009) 765-770.
14. R.A. Shakoor, R. Kahraman, U. Waware, Y. Wang, W. Gao, *Mater. Des.*, **64** (2014) 127-135.
15. B. Kaya, T. Gulmez and M. Demirkol, *AIP Confer. Proceedings.*, **1127** (2009) 62-73.
16. R. A. Shakoor, R. Kahraman, U. S. Waware, Y. Wang, W. Gao, *Int. J. Electrochem. Sci.*, **10** (2015) 2110 – 2119.
17. Y..N. Bekish, S.K. Poznyak, L.S. Tsybulskaya, T.V. Gaevsкая. *Electrochim. Acta.*, **55** (2010) 2223-2231.
18. D. S. Jayakrishnan, 5 - Electrodeposition: the versatile technique for nanomaterials, in *Corrosion Protection and Control Using Nanomaterials*, V.S. Saji and R. Cook, Editors. *Woodhead Publishing.*, (2012) 86-125.
19. I.G.a.L. Binder, *Sci. Technol. Adv. Mater.*, **9** (2008) 1-11.
20. C. R. Pichard, Z. Bouhala, A. J. Tosser, A. Rashid, J. Flechon, *J. Mater. Sci.*, **20** (1985) 3305-3310.
21. K.H. Lee, D. Chang and S.C. Kwon, *Electrochim. Acta.*, **50** (2005) 4538-4543.
22. T.V. Gaevsкая, I.G. Novotortseva and L.S. Tsybulskaya, *Metal Finishing.*, **94** (1996) 100-103.
23. S.M.A. Shibli and J.N. Sebeelamol, *Int. J. Hydrogen Energy.*, **38** (2013) 2271-2282.
24. S.M.A. Shibli, N.D. Suma, and V.S. Dilimon, *Sensors and Actuators B: Chemical.*, **129** (2008) 139-145.
25. M. Alizadeh, M. Mirak, E. Salahinejad, M. Ghaffari, R. Amini, A. Roosta, *J. Alloys and Compd.*, **611** (2014) 161-166.
26. K. Krishnaveni, T.S.N. Sankara Narayanan and S.K. Seshadri, *Surf. Coat Technol.*, **190** (2005) 115-121.
27. Z.A. Hamid, H.B. Hassan and A.M. Attyia, *Surf. Coat Technol.*, **205** (2010) 2348-2354.
28. C.T. Dervos, J. Novakovic and P. Vassiliou, *Mater. Lett.*, **58** (2004) 619-623.
29. K.M. Gorbunova, M.V. Ivanov and V.P. Moiseev, *J. The Electrochem. Soc.*, **120** (1973) 613-618.
30. N.S. Qu, D. Zhu and K.C. Chan, *Scripta Materialia.*, **54** (2006) 1421-1425.

31. C. D. Ríos, A.H. Macias, R. Torres-Sánchez, M.A. Ramos, and J.G. Hernández, *Industrial & Engineering Chemistry Research.*, 51 (2012) 7762-7768.
32. S. Yuan, S.O. Pehkonen, B. Liang, Y.P. Ting, K.G. Neoh, E.T. Kang, *Corros. Sci.*, 53 (2011) 2738-2747.

© 2015 The Authors. Published by ESG ([www.electrochemsci.org](http://www.electrochemsci.org)). This article is an open access article distributed under the terms and conditions of the Creative Commons Attribution license (<http://creativecommons.org/licenses/by/4.0/>).